

# The Effect of Platelet-Rich Plasma and/or Pentoxifylline on Experimentally Induced Achilles Tendon Injury in Adult Male Albino Rats

Original  
Article

Adham Abdelrahman<sup>1</sup>, Salwa Saeed El Sabeh<sup>1</sup>, Eman Elazab Beheiry Elazab<sup>1</sup>, Sally Mahmoud Mohamed Hussein Omar<sup>1</sup> and Dina M. Rostom<sup>2</sup>

<sup>1</sup>Department of Anatomy and Embryology, <sup>2</sup>Department of Histology and Cell Biology, Faculty of Medicine, Alexandria University, Egypt

## ABSTRACT

**Introduction:** Achilles tendon injury is common in athletic men. Surgical repair is the usual line of management; however, other lines of treatment were adopted. Platelet-rich plasma (PRP) contains growth factors that accelerate healing. Pentoxifylline (PTX) improves healing by increasing tissue perfusion through vasodilatation.

**Objective:** The aim of the present work was to elucidate the effect of PRP and PTX either alone or in combination on the healing process of injured Achilles tendon in adult male albino rats by histological, morphometric and biomechanical studies.

**Materials and Methods:** Ninety-five healthy laboratory adult male albino rats. Five rats were used as platelet-rich plasma donors. Ninety rats were divided into 5 groups 18 rats each; Group I: control group, Group II: injured untreated group, Group III: received local PRP injection into the operation site, Group IV: received daily IM PTX injections, Group V: combination group received both PRP and PTX. On day 15, the Achilles tendon of eight rats from each group was dissected. Five tendons were used in the light microscopic study and the other three were used in the ultrastructural study by scanning electron microscope to assess the structural properties of the tendon. On day 30, the Achilles tendon of ten rats from each group was dissected. Five tendons were used for the morphometric study while the other five were used for the biomechanical study to assess the functional properties of the tendon.

**Results:** Combined PRP + PTX treated group V showed better healing results than all other experimental groups both histologically and biomechanically. PRP-treated group III showed better healing than PTX-treated group IV which in turn was superior to the untreated group II.

**Conclusion:** There is a benefit of using combined PRP and PTX than either treatment alone in promoting Achilles tendon healing post-injury.

**Received:** 12 July 2023, **Accepted:** 11 August 2023

**Key Words:** Achilles tendon, pentoxifylline, platelet-rich plasma.

**Corresponding Author:** Adham Abdelrahman, PhD, Department of Anatomy and Embryology, Faculty of Medicine, Alexandria University, Egypt, **Tel.** +2 012 7746 3146, **E-mail:** elmallahadham@gmail.com

**ISSN:** 1110-0559, Vol. 47, No. 3

## INTRODUCTION

Achilles tendon (AT) injury is among the most prevalent musculoskeletal injuries generally occurring in middle-aged athletic men<sup>[1-4]</sup>. It has a rate of incidence of 18 per 10,000 individuals worldwide with a constant rise, affecting up to one million athletes each year<sup>[5]</sup>. It is also considered the most encountered tendon injury in the lower limb<sup>[6]</sup>.

Sudden violent dorsiflexion of a plantar flexed ankle during vigorous exercises is the most commonly reported mechanism for Achilles tendon rupture<sup>[7]</sup>. Owing to the hypovascularity and the hypocellularity of tendons, they have a limited and inefficient healing capacity. This explains the fact that the injured tendon rarely gains the original biological and mechanical properties post-healing<sup>[8]</sup>.

Many surgical and non-surgical treatment options have been tried to improve final outcomes both structurally and functionally. However, the treatment options are usually unsatisfactory and often lead to limitations such as delayed return to work and extended periods of inability to participate in sports, thus affecting the normal quality of life. Therefore, it is beneficial to search for new treatment options to expedite recovery and improve tissue repair quality<sup>[9]</sup>.

One of the promising used treatments is platelet-rich plasma (PRP) injection, being a minimally invasive, cheap, simple and effective treatment option<sup>[10-12]</sup>. Platelet-rich plasma is becoming more popular as an adjuvant product derived from human blood to possibly improve the healing process and modulate inflammation. Since it has shown effectiveness in ameliorating various health conditions such

as osteoarthritis, skin aging and skin wound healing[6]. In addition, PRP was used as an adjuvant treatment option for various musculoskeletal injuries including acute tendon rupture, ligament sprains, muscle injury and articular cartilage injury<sup>[13-16]</sup>.

Despite the fact that there are several published clinical research on the applications of PRP in injuries of the musculoskeletal system, its efficacy is yet unclear, making its use controversial<sup>[17,18]</sup>.

Another promising healing booster is pentoxifylline (PTX) which has shown success in promoting healing in intractable ulcers, burns and skin wounds. Being a vasodilator, it improves peripheral circulation which in turn increases tissue perfusion and accelerates the healing process. With few reported side effects, it is generally tolerated by most of the patients<sup>[19,20]</sup>.

The present work aims to elucidate and compare the effect of platelet-rich plasma and pentoxifylline, either used separately or in combination, on the healing process of induced Achilles tendon injury in adult male albino rats by morphometric, histological and biomechanical studies.

## MATERIALS AND METHODS

### Materials

#### Chemicals

- Pentoxifylline (Trentoximal 100 mg/5ml ampoules, Alex /Egypharma Co.).
- Platelet-rich plasma (PRP).
- Ketamine 50 mg/ml (Ketam 50 mg/ml vial, Eipico co.) was obtained from Alexandria main university hospital's pharmacy and used for anesthesia.
- Povidone-Iodine solution 10% (Betadine antiseptic solution 10%, Mundipharma Co.) used for skin disinfection.
- Ceftriaxone sodium 250 mg vial (Ceftriaxone 250 mg, Sandoz Co.) used for surgical prophylaxis against infection.
- Acetaminophen 10 mg/ml vial (Perfalgan 10mg/ml vial, BMS Co.) used for postoperative analgesia.

#### Experimental Animals and treatment

The study was performed on 95 healthy adult male albino rats. The rats were provided by the Animal house center, Faculty of Medicine, Alexandria University. Their weight range was from 200 to 250 g. Before the experiment, the animals were given two weeks to acclimatize. They were kept under a standard laboratory environment of humidity, temperature and 12-hour light/dark cycle. Food and water were given to the animals ad libitum during the period of the experiment. Guidelines for care and use of animals, approved by the Research Ethics Committee, Faculty of Medicine, University of Alexandria were followed.

The rats were divided into: (Figure 1)

- Platelet-rich plasma donor group: included five rats.
- Experimental study animals: included 90 rats, which were divided into five groups, 18 rats each;

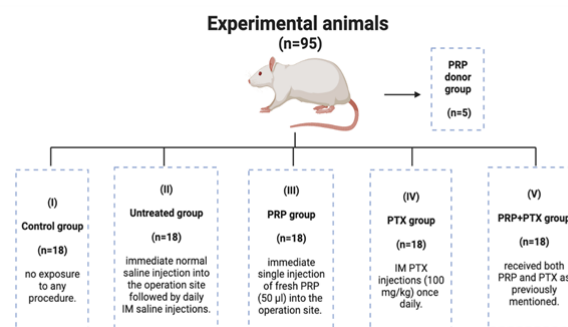


Fig. 1: A diagram showing experimental animals and grouping

**Group I (Control group):** weren't exposed to any procedure.

**Group II (Untreated injured group):** received local normal saline injections into the sutured operation site immediately after the operation of Achilles tendon injury, followed by intramuscular normal saline injections daily for 15 days (8 rats) and 30 days (10 rats).

**Group III (PRP group):** received a single freshly prepared PRP (50 µl) injection into the sutured operation site immediately after the operation<sup>[21]</sup>.

**Group IV (PTX group):** received pentoxifylline intramuscular injections (100 mg/kg) once daily,<sup>[2]</sup> starting from the day of the operation, for 15 days (8 rats) and 30 days (10 rats).

**Group V (Combined PRP + PTX group):** received injections of both PRP injection and pentoxifylline as previously mentioned in group III and group IV respectively.

### Methods

#### Platelet-rich plasma (PRP) preparation

The PRP was prepared at the Department of Medical Biochemistry, Faculty of Medicine, Alexandria University. Whole blood was obtained from the donor group (five adult male albino rats). The blood was centrifugated at 400 g (relative centrifugal force) for 10 minutes. In another tube, the supernatant was transferred and re-centrifugated at 800 g for 10 minutes<sup>[22]</sup>. The upper two thirds of the tube (Platelet-poor plasma) were discarded, while the lower third was considered as platelet-rich plasma (PRP)<sup>[23,24]</sup>.

#### Induction of Achilles tendon injury

Induction of Achilles tendon injury was done under general anaesthesia using 10% Ketamine HCL 50 mg/kg IM<sup>[1]</sup>. After shaving the skin of the right hindlimb by a

razor, the area of surgery was disinfected using povidone-iodine. A 1.5 cm longitudinal surgical incision of the skin was made over the Achilles tendon. After exposure of the Achilles tendon, the plantaris tendon was identified and removed using a pair of scissors<sup>[9]</sup>. A full-thickness horizontal incision was performed on the tendon by a scalpel 0.5 cm above the calcaneus insertion area<sup>[25]</sup>. The incised tendon was immediately repaired by simple sutures and the skin wound was stitched using prolene 4/0 sutures. (Figure 2) Postoperative analgesia (acetaminophen 50 mg/kg SC), prophylactic antibiotic (ceftriaxone 50mg/kg IM) and wound care were implemented<sup>[1]</sup> The day of this surgical procedure was considered day 0. Postoperatively, the rats were allowed to move freely<sup>[1,26]</sup>.

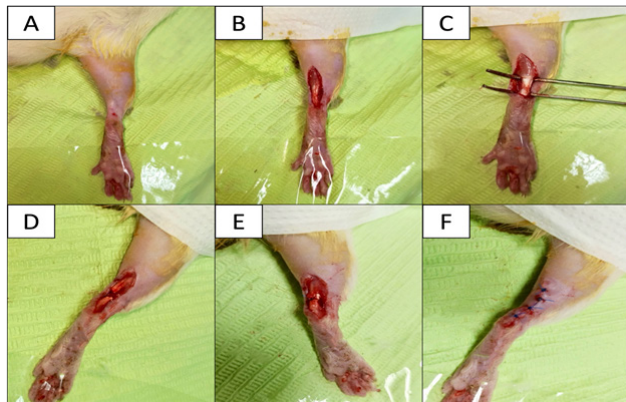


**Fig. 2:** Photographs showing steps of induction of Achilles tendon injury. A: Skin of right hindlimb was shaved and disinfected with povidone iodine B: A 1.5 cm longitudinal incision was made proximal to the calcaneus. C: Achilles tendon was identified and dissected. D: A transverse incision was made in the tendon 0.5 cm above its insertion. E: The tendon was sutured using prolene 4/0 sutures. F: Skin was closed using prolene 4/0

### ***Achilles tendon healing assessment***

On day 15, eight rats from each group were operated on under light ether anaesthesia<sup>[27]</sup> The Achilles tendon was dissected and prepared for histological examination. Five tendons were used in the light microscopic study and the other three were used in the ultrastructural study by scanning electron microscope. On day 30, the rest ten rats of each group were operated on under light ether anaesthesia<sup>[27]</sup>. The Achilles tendon was dissected and prepared for morphometric and biomechanical evaluation. Five tendons were used for the biomechanical study while the other five were used for the morphometric study.

### ***Histological study***

#### ***Light microscopic study***

To examine the histological changes, 10% neutral buffered formalin was used to fix the tendon specimens for preparing the paraffin sections<sup>[20,28,29]</sup>. Sections were obtained from paraffin blocks (5 to 6µm-thick) and were prepared using standardized tissue processing techniques. The stains used were:

- Hematoxylin and eosin (H & E) stain.

- Masson's trichrome stain for assessment of collagen fibers density.
- Alcian blue with Periodic acid-Schiff (PAS) stain for assessment of the ground substance.

The samples were scored according to Bonar histological grading scale<sup>[4]</sup>. Four variables were scored in the Bonar system: tenocytes, ground substance, collagen and vascularity. A four-point scoring system was used, from 0 to 3, 0 indicates a normal histological appearance, while 3 indicates a severely abnormal one. For each specimen, the total score ranged from 0 (normal tendon structure) to 12 (the most severe abnormality). It means that higher scores indicate poorer tendon healing. Scoring was performed by 2 blinded observers<sup>[4,29,30]</sup>.

- ImageJ computer software was used to quantify the blue color intensity of Masson's trichrome as well as Alcian blue/PAS-stained sections.
- The data was based on the mean number and tabulated.

### ***Ultrastructural study***

Tendon specimens were extracted and fixed by immediate immersion in 4F1G (4% formaldehyde and 1% glutaraldehyde) in 0.1M buffer of pH 7.2 at 4° C for 2-24 hours followed by washing the specimens in distilled water then dehydration using graded ethanol. The specimens were allowed to dry then were coated with gold A in a sputter-coating unit (JFC-1100 E). Morphology in the coded specimens was examined and photographed by a JEOL scanning electron microscope (SEM) (JSM- IT200, In Touch Scope Series) at the Electron Microscopy Unit, Faculty of Science, Alexandria University<sup>[31-33]</sup>.

### ***Morphometric study***

A 2 mm cross-sectional tendon segment was resected including the suture line. The tendon segment was examined and photographed using Olympus SZ Dissecting Stereo Microscope at the department of Human Anatomy and Embryology, Faculty of Medicine, Alexandria University. Three anthropometric measures of the tendon segment were obtained using computer-assisted image analysis; the width (w) (maximum mediolateral diameter), the thickness (t) (maximum anteroposterior diameter), then the cross-sectional area (A) was calculated<sup>[34]</sup>.

### ***Biomechanical study***

The tendons and paratenons were excised including part of gastrocnemius & soleus muscles proximally and the calcaneus distally<sup>[28]</sup>. All specimens were soaked in 0.9% saline solution and kept in the freezer at -20 °C till the day of the test<sup>[28,35]</sup>. On the day of the test, the specimens were allowed to thaw at room temperature<sup>[27]</sup>. The tendons' tensile strength, expressed in Newtons, was measured using Mecmesin MultiTest 5-XT Tension and Compression Testing System at Materials engineering laboratory, Faculty of Engineering, Alexandria University



(Figure 3). The upper and lower jaws of the device were applied to the two ends of the specimen. The load value was increased by the device at 10 mm/min pulling speed till the specimen ruptured. At this point, the load at failure (Fmax) was recorded by computer software connected to the device<sup>[27,28]</sup>.



**Fig. 3:** A photograph of Mecmesin MultiTest 5-XT Tension and Compression Testing System

### Statistical analysis

Data was analyzed using IBM SPSS software package version 20.0. Quantitative data was described using range (minimum and maximum), mean, standard deviation and median. A *p*-value of <0.05 was considered statistically significant. F-test (ANOVA) was used to compare between the studied groups for normally distributed quantitative variables and Post Hoc test (Tukey) was used for pairwise comparisons. Abnormally distributed quantitative variables were tested using Kruskal Wallis test to compare between the studied groups and Post Hoc (Dunn's multiple comparisons test) was used for pairwise comparisons<sup>[36,37]</sup>.

## RESULTS

No deaths among experimental animals have been recorded.

### Histological results

#### Light microscopic results

##### H & E stain

Longitudinal sections of normal rat Achilles tendon group I (control group) showed uniformly arranged slightly wavy collagen fibers packed in tightly cohesive well demarcated bundles running parallel to one another and to the long axis of the tendon. No blood capillaries

were identified within the tendon tissue. The paratenon is composed of loose areolar connective tissue of normal appearance and thickness (Figure 4A). At higher magnification, tenocytes were arranged longitudinally and appeared spindle shaped with elongated nuclei and without obvious cytoplasm. (Figure 4B). Histological sections of group II (untreated injured group) at the repair site showed distorted tendon tissue architecture, collagen fibers appeared running in different directions, numerous tissue gaps were recognized in addition to inflammatory cell infiltration was seen all over the injury site mainly at the tendon-paratenon interface. Areas of hemorrhage, adipocytes infiltration were identified. The paratenon appeared with apparently wide spaces and infiltrated with mononuclear inflammatory cells (Figure 5A). Higher magnification showed loss of demarcation between collagen fibers and clusters of capillaries (Figure 5B). Hypercellularity was observed where tendon cells acquired rounded nuclei and visible cytoplasm (Figure 5B). Sections of group III (PRP group) showed mild distortion of tendon tissue architecture. Most of the collagen fibers appeared running parallel to each other in bundles. Mild inflammatory infiltrate was recognized along with few discrete blood capillaries (Figure 5C). The paratenon appeared mildly thickened with hypercellularity (Figure 5C inset). At higher magnification, collagen fibers show increased undulation. Hypercellularity was observed and the tendon cells acquired oval shape with oval nuclei with visible basophilic cytoplasm (Figure 5D). In group IV (PTX group), there was mild distortion of tendon tissue architecture. Most of the collagen fibers appeared parallel to each other. Mild inflammatory infiltrate was observed predominantly at the paratenon-tendon interface (Figure 6A inset). Numerous discrete capillaries were identified (Figure 6A) Evident hypercellularity with tendon cells nuclei appearing rounded to oval with barely visible cytoplasm was visualized (Figures 6 A,B). The paratenon appeared thickened with scattered capillaries (Figure 6A inset). At the repair site of group V (combined group), the tendon showed nearly restored tissue architecture with minimal distortion. Collagen fibers appeared wavy and well-demarcated. Mild inflammatory infiltrate was observed (Figure 6C). The paratenon appeared of normal thickness with numerous discrete capillaries aligned at the paratenon-tendon interface (Figure 6C). At higher magnification, collagen fibers appeared well demarcated with increased undulation. Hypercellularity was recognized with most of the tendon cells acquiring an elongated fusiform shape with inconspicuous cytoplasm (Figure 6D).

##### Masson's trichrome stain

Masson's trichrome staining of normal tendon group I (control group) demonstrated organized bundles of parallel blue stained collagen fibers. Tenocytes were scanty. No visible blood vessels (Figure 7A). Tendon sections of group II (untreated injured group) showed distortion of normal tendon tissue architecture with faint blue staining of collagen fibers. Hypercellularity, tissue gaps, clusters of capillaries and adipocyte infiltration were recognized

(Figure 7B). Sections of group III (PRP group) showed mild distortion of tendon tissue architecture, moderately intense blue staining of collagen fibers. Hypercellularity and discrete capillaries were seen (Figure 7C). Group IV (PTX group) showed mild distortion of normal tendon tissue architecture with collagen blue staining of moderate intensity. Hypercellularity and numerous discrete capillaries were observed (Figure 7D). Group V (combined group) showed restored tendon tissue architecture and intense blue staining of collagen fibers. Hypercellularity and few discrete capillaries were identified (Figure 7E). Different studied groups were compared according to blue color staining intensity by Masson's trichrome using ImageJ software (Figure 7F).

#### **Alcian blue/PAS stain**

Alcian blue/PAS staining of normal tendon (group I) showed normal tendon tissue architecture with discrete collagen fibers stained red with PAS. Scanty ground substance stained blue by Alcian blue could be visualized between discrete fibers (Figure 8A). Contrarily, sections of group II at the injury site showed evident distortion of normal tendon tissue architecture with loss of demarcation between collagen fibers and abundant stainable ground substance in between (Figure 8B). Stained tendon sections of group III showed well-preserved tendon tissue architecture with wavy collagen fibers and mild blue ground substance in between fibers (Figure 8C). Stained tendon sections of group IV showed mild distortion of tendon tissue architecture with a moderate Alcian blue staining of the ground substance in between fibers (Figure 8D). Stained tendon sections of group V showed restored tendon tissue architecture with minimal ground substance between parallel fibers (Figure 8E). The different studied groups were compared according to blue color staining intensity by Alcian blue using ImageJ software (Figure 8F).

A comparison between the different studied groups was performed according to the mean of Bonar score (Table 1, Figure 9).

#### **Electron Microscopic results**

Under the scanning electron microscope, the tendon tissue segments of group I (control group) showed regular alignment of mature collagen fibers in longitudinal sections. The fibers were bundled and run parallel to one another and to the long axis of the tendon, there was no gapping within the tissue between the fibers with absence of immature collagen fibers. Cross section showed tightly packed collagen bundles with normal fiber thickness and density (Figure 10A). On the other hand, longitudinal sections of the untreated group II at the repair site showed irregular arrangement of the collagen fibers which run

in different directions as well as the predominance of randomly oriented loosely arranged collagen fibers split into kinked broken intermingled immature fibers which give a lacy appearance. In cross sections the collagen fibers appeared thin, sparsely distributed and irregularly arranged with abundant spaces between the bundles (Figure 10B). In longitudinal section of group III (PRP group), a well-preserved tendon architecture was observed. The collagen fibers acquired a uniform axial orientation. Fibers showed a smooth undulated pattern with increased bundling and decreased tissue gaps. High mature to immature collagen ratio was observed. Increased fiber density and thickness were recognized in cross sections. Collagen was arranged in packed bundles with minimal gaps in between (Figure 10C). In group IV (PTX group), the collagen fibers began to form an axial arrangement and were almost wavelike. There was an increase in the density of mature collagen fibers at the expense of immature thin lacy collagen fibers. Although gapping was still present between the fibers, more packing of fibers into bundles have been observed in cross sections as well as increase in density and thickness of individual collagen fibers (Figure 10D). Sections of group V (combined group) showed a well-preserved tendon architecture. The collagen fibers acquired a uniform axial orientation. Fibers showed a smooth undulated pattern with increased bundling and decreased tissue gaps. Mature to immature collagen ratio has much increased. Increased fiber density and thickness was recognized in cross sections. Collagen was arranged in packed bundles with minimal gaps in between (Figure 10E).

#### **Morphometric results**

By examining the tendon segments on day 30 under the Olympus dissecting microscope, the segments appeared round to oval in shape with the paratenon at the periphery giving the specimen an irregular outline. The difference between groups regarding the general gross morphology of the tendon tissue was non-significant. All tendon segments attained almost the same width, thickness and cross-sectional area. The statistical differences between groups were minimal and insignificant ( $p > 0.05$ ) (Table 2, Figure 11).

#### **Biomechanical results**

At day 30 post-injury, the mean of the recorded maximum load values (Fmax) in group V (mean Fmax = 6.28) was significantly higher than all other injured groups and it approached those recorded in the control group I (mean Fmax = 7.72). The Fmax values of group III (mean Fmax = 5.36) were significantly higher than group IV (mean Fmax = 3.78). The mean value of the latter group was slightly higher than the untreated injured group II (mean Fmax = 3.10) (Table 3, Figure 12).



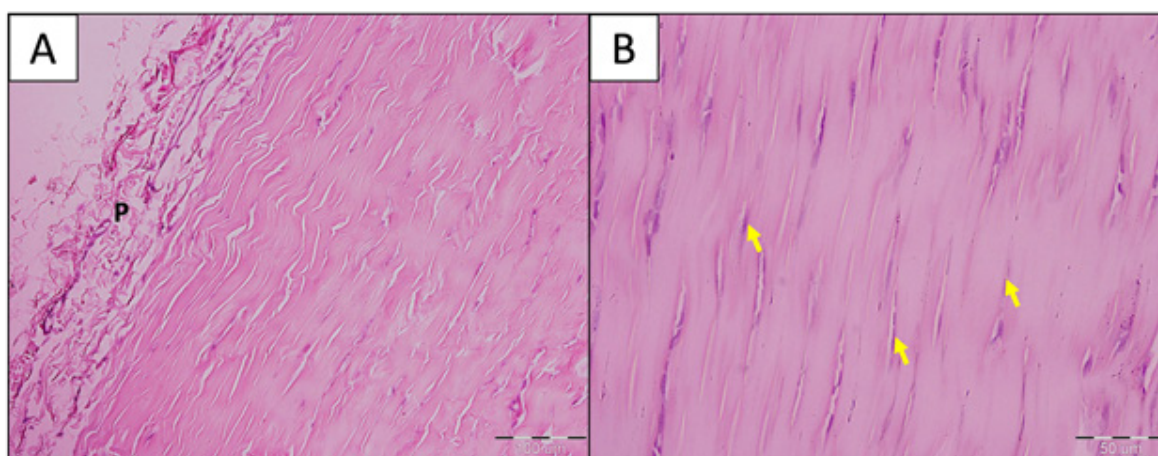


**Fig. 4:** Photomicrographs of normal rat's Achilles tendon (control group I) A: Showing normal tendon architecture of uniformly arranged slightly wavy collagen fibers packed in tightly cohesive well-demarcated bundles running parallel to each other and to the longitudinal axis of the tendon. B: Tenocytes (yellow arrows) are spindle shaped with elongated nuclei. The loose areolar tissue of the paratenon (P) shows normal appearance and thickness. (H&E stain Mic. Mag. A X200, B X400)

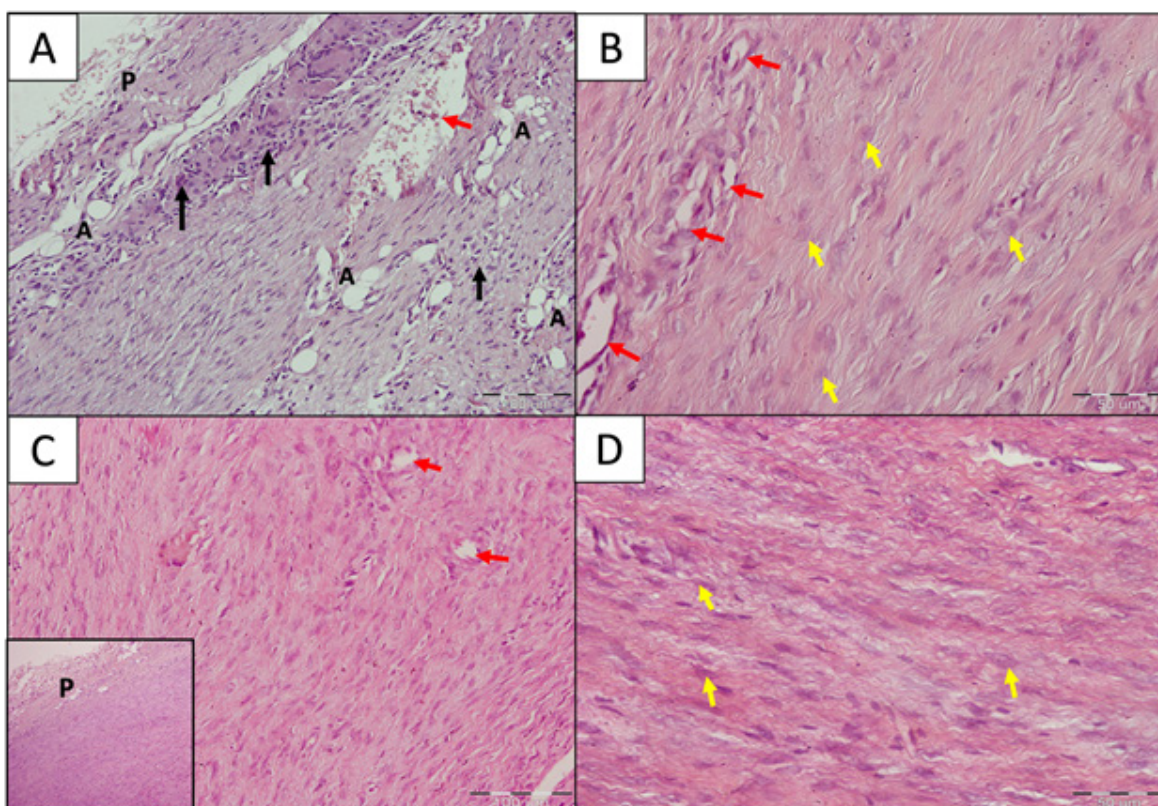


**Fig. 5:** Photomicrographs of rat's Achilles tendon at the site of induced injury. A: Untreated injured group (II), showing distorted tissue architecture, increased thickness and cellularity of the paratenon (P) with mononuclear inflammatory cellular infiltration at the tendon-paratenon interface (black arrows). The paratenon appeared with apparently wide spaces. Note the areas of adipocyte cellular infiltration at (A). Areas of hemorrhage (red arrow) were seen. B: Untreated injured group (II) at higher magnification showing loss of demarcation between collagen fibers as well as clusters of capillaries (red arrows). Hypercellularity with tendon cells nuclei appear rounded in shape with visible cytoplasm (yellow arrows). C: PRP group (III) showing mild distortion of normal tissue architecture, collagen fibers show axialization and run parallel to each other, hypercellularity with cells appearing oval. Few discrete capillaries can be seen (red arrows). Inset: paratenon (P) appears moderately thickened with hypercellularity. D: PRP group (III) at higher magnification showing well demarcated deeply stained parallel collagen fibers with wavy appearance and slight separation of bundles. Hypercellularity with tendon cells nuclei appear oval in shape with visible basophilic cytoplasm (yellow arrows). (H&E stain Mic. Mag. A & C X200, B & D X400, inset X100)

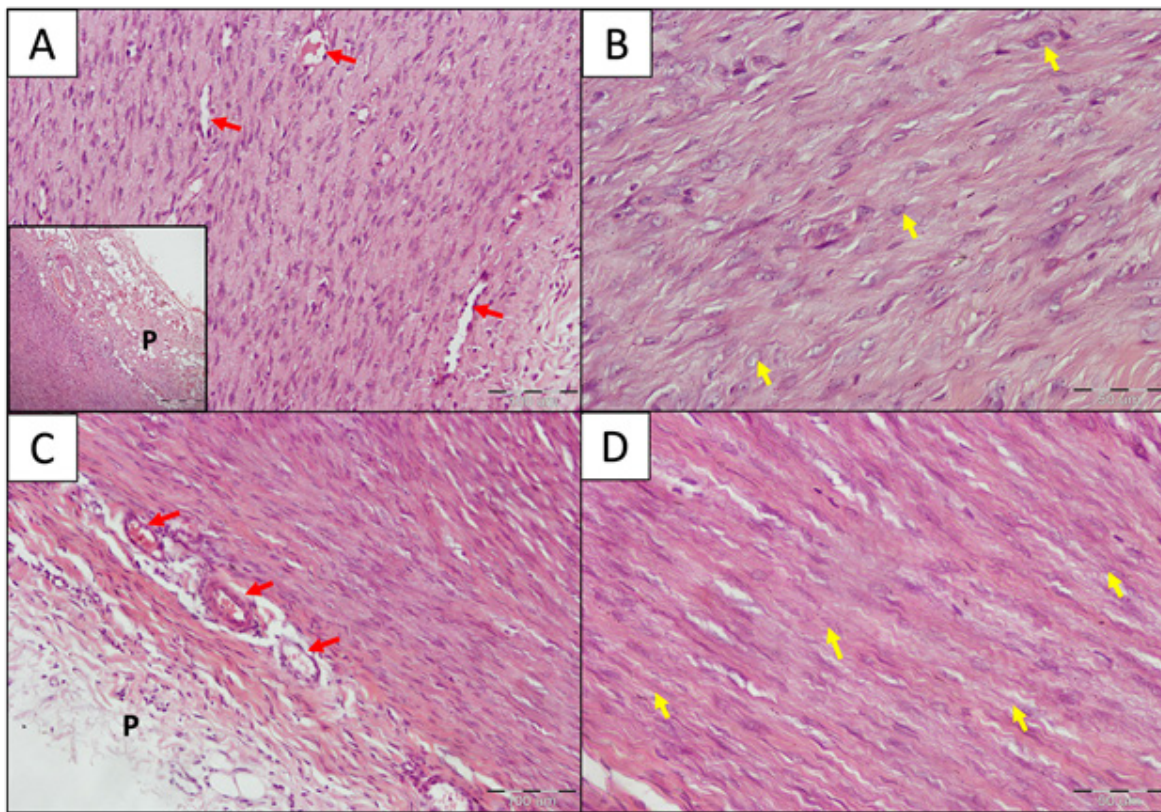


**Fig. 6:** Photomicrographs of rat's Achilles tendon at the site of induced injury. A: PTX group (IV) showing mild distortion of normal tissue architecture, evident hypercellularity with numerous scattered capillaries (red arrows). Inset: Paratenon (P) appears edematous with hypercellularity and multiple scattered capillaries. B: PTX group (IV) at higher magnification showing well demarcated parallel collagen fibers with wavy appearance. Hypercellularity is seen with tendon cells nuclei appear oval to rounded in shape with small amount of cytoplasm (yellow arrows). C: PRP + PTX group (V) showing well restored tendon tissue architecture. Collagen fibers are tightly cohesive running parallel to each other and to the longitudinal axis of the tendon. Paratenon (P) appears of normal thickness. Hypercellularity with numerous discrete capillaries aligned at the paratenon-tendon interface (red arrows). D: PRP + PTX group (V) at higher magnification showing well demarcated parallel collagen fibers with wavy appearance. Hypercellularity with tendon cells nuclei appear pale oval to fusiform in shape with conspicuous cytoplasm (yellow arrows). (H&E stain Mic. Mag. A & C X200, B & D X400, inset X100)



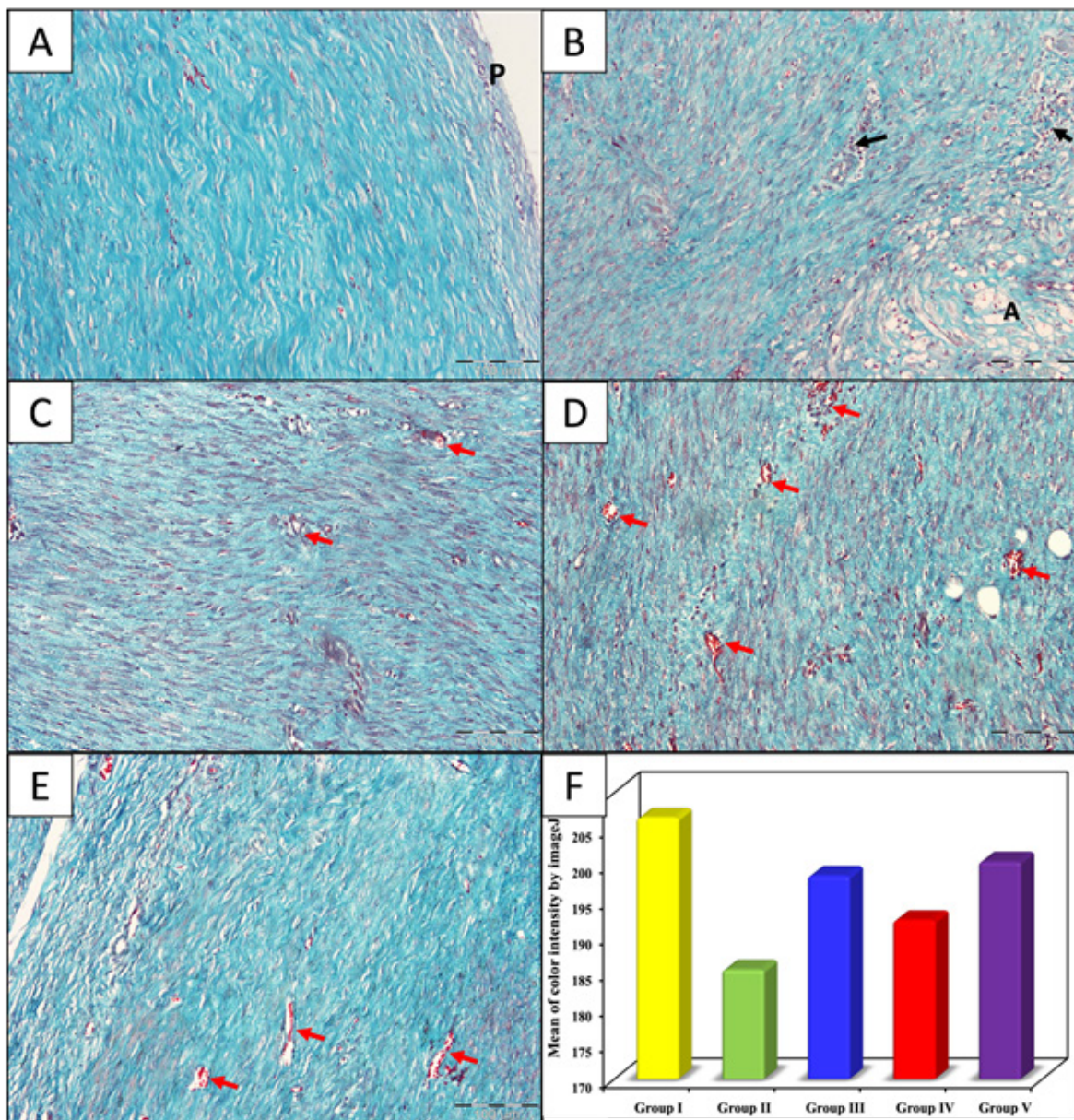


**Fig. 7:** Photomicrographs of rat's Achilles tendon A: Control group (I) near the paratenon showing intense regular collagen staining. Collagen fibers are arranged in tightly cohesive well demarcated bundles. B: Untreated injured group (II) at site of induced injury showing low staining intensity of collagen, loss of normal tendon tissue architecture where collagen fibers run in different directions with loss of demarcation between them. Note the inflammatory infiltrate (black arrows) and adipose infiltration (A). C: PRP group (III) showing increased staining intensity of collagen, mild distortion of tissue architecture with evident hypercellularity. Few discrete capillaries can be seen (red arrows). D: PTX group (IV) showing increased staining intensity of collagen, mild distortion of tissue architecture with unclear demarcation between collagen fibers. Evident hypercellularity was recognized. Note the numerous discrete capillaries (red arrows). E: PRP + PTX group (V) showing increased staining intensity of collagen with apparent restoration of the normal architecture. Slight separation of individual collagen fibers but maintained well demarcated bundles was noticed. Few Discrete capillaries can be seen (red arrows). F: A bar chart showing comparison between different studied groups according to blue color staining intensity by Masson's trichrome using ImageJ software. (Masson's trichrome stain Mic. Mag. X200)



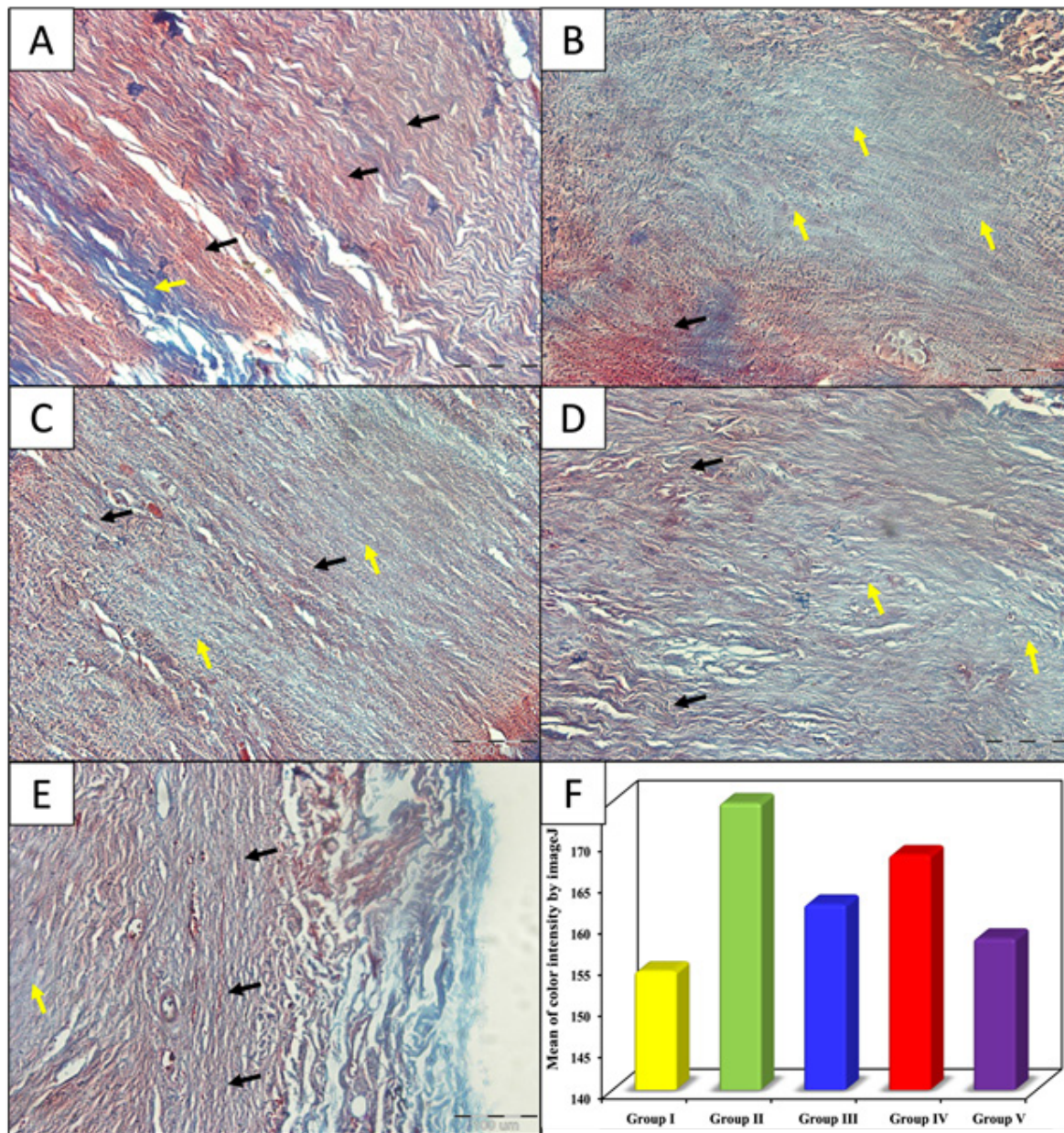


**Fig. 8:** Photomicrographs of rat's Achilles tendon. A: Control group (I) showing normal tendon tissue architecture with scanty blue stainable ground substance between discrete collagen fibers. B: Untreated injured group (II) at the site of induced injury showing distorted tendon tissue architecture with loss of demarcation between collagen fibers. Abundant ground substance was stained blue with Alcian blue between fibers. C: PRP group (III) showing well-preserved tendon tissue architecture with wavy appearance of collagen fibers. Mild blue staining of ground substance can be visualized between fibers. D: PTX group (IV) showing moderate blue staining of ground substance between collagen fibers. Tendon tissue architecture is mildly distorted. E: PRP + PTX group (V) showing well-preserved tissue architecture with discrete parallel collagen fibers. Faint blue staining of ground substance appears within the tendon tissue and accentuated at the paratenon (P). Black arrows point to collagen fibers, yellow arrows point to Alcian blue-stained ground substance. F: A bar chart showing comparison between different studied groups according to blue color staining intensity by Alcian blue using ImageJ software. (Alcian blue/PAS stain Mic. Mag. X200)

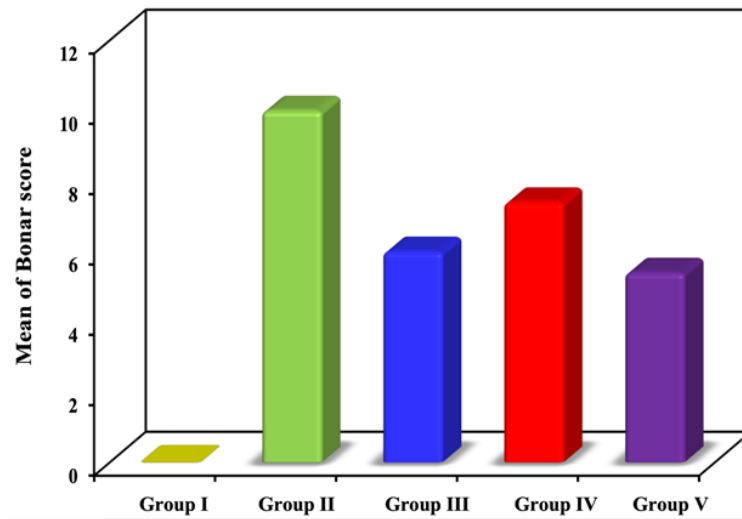


Fig. 9: A bar chart showing comparison between the different studied groups according to mean of Bonnar Score

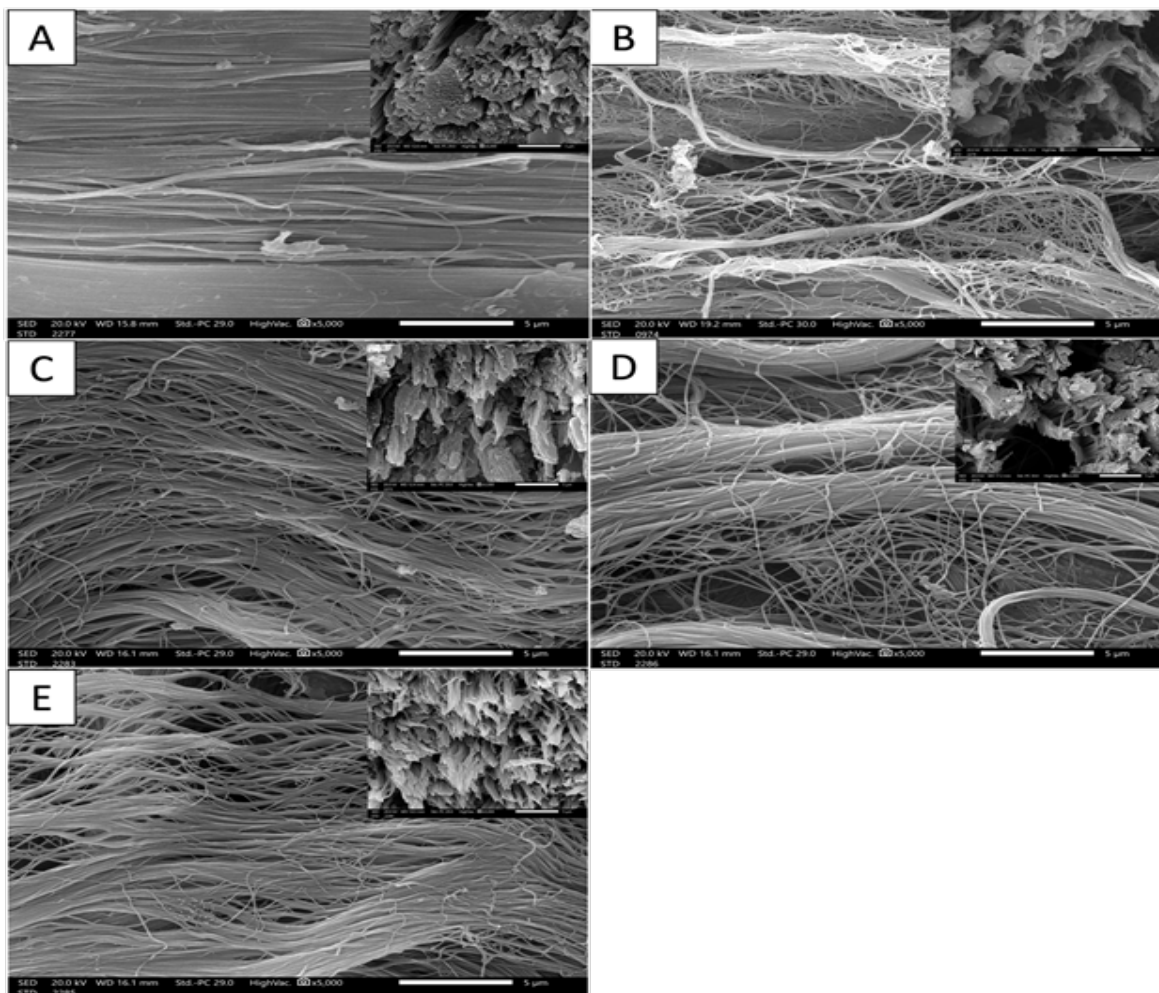


Fig. 10: Electron photomicrographs of rat's Achilles tendon. A: Control group (I) showing regular arrangement of parallel mature collagen fibers in bundles with no gaps in longitudinal section. Collagen fibers appear tightly bundled with normal thickness and density in cross section (inset). B: Untreated injured group (II) showing abundant randomly oriented loosely arranged collagen fibers split into kinked broken intermingled immature fibrils running in different directions giving a lacy appearance with loss of normal tendon architecture. Collagen fibers appear sparse with much gapping between bundles in cross section (inset). C: PRP group (III) showing increased axialization of collagen fibers arranged in uniform undulated bundles with increase mature to immature collagen ratio. Collagen bundles appear dense and more packed with less tissue gaps in cross section (inset). D: PTX group (IV) showing collagen fibers began to acquire an axial arrangement. More high-density mature collagen fibers arranged in bundles is observed with less tissue gaps between bundles in cross section (inset). Other fibers appear thin and have a reticular arrangement. E: PRP + PTX group (V) showing collagen fibers with evident axialization and bundling. Collagen bundles appear undulated and tightly packed with increased fiber density and minimal tissue gaps in cross section (inset). (Mic. Mag. X5000, inset X5000)



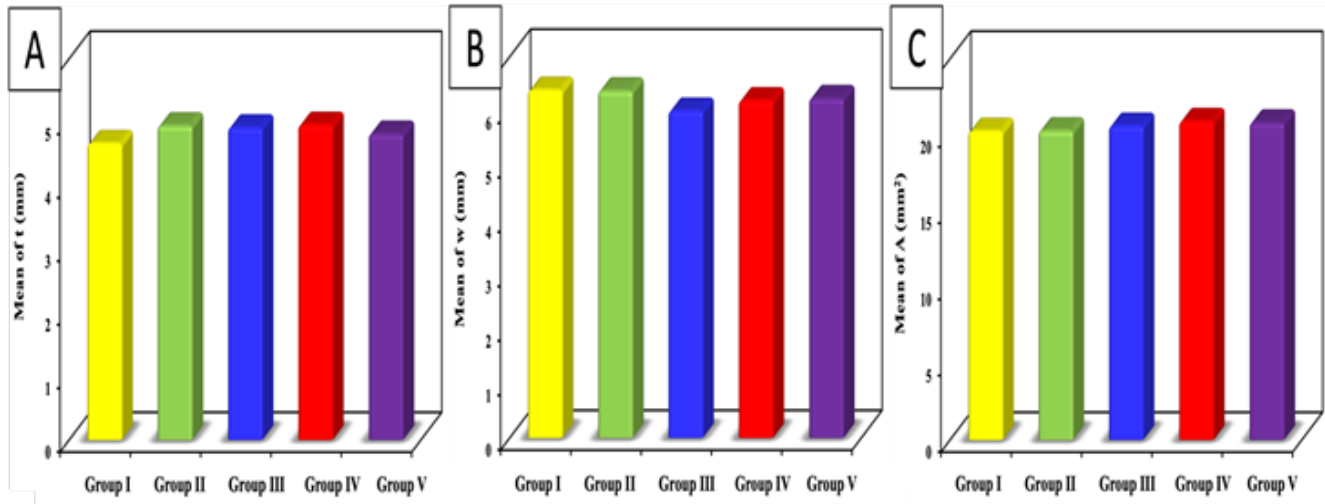


Fig. 11: A: A bar chart showing comparison between the different studied groups according to mean of t (mm). B: A bar chart showing comparison between the different studied groups according to mean of w (mm). C: A bar chart showing comparison between the different studied groups according to mean of A (mm<sup>2</sup>)

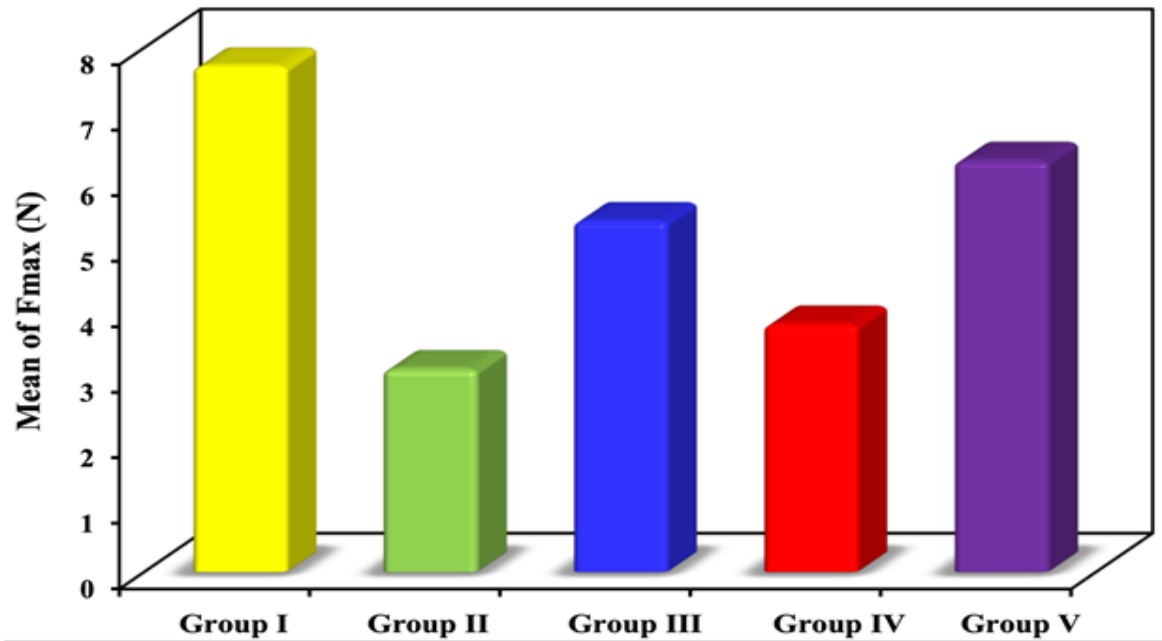


Fig. 12: A bar chart showing comparison between the different studied groups according to mean of Fmax

**EFFECT OF PRP AND PTX ON ACHILLES TENDON INJURY**

**Table 1:** comparison between the different studied groups according to Bonar score.

| Bonar score             | Group I (n = 5) | Group II (n = 5) | Group III (n = 5)   | Group IV (n = 5) | Group V (n = 5) | Test of Sig. | p       |
|-------------------------|-----------------|------------------|---|------------------|-----------------|--------------|---------|
| <b>Tenocytes</b>        |                 |                  |   |                  |                 |              |         |
| Min. – Max.             | 0.0 – 0.0       | 2.0 – 3.0        | 1.0 – 2.0   | 2.0 – 2.0        | 1.0 – 2.0       | H= 20.021*   | <0.001* |
| Mean ± SD.              | 0.0 ± 0.0       | 2.60 ± 0.55      | 1.40 ± 0.55   | 2.0 ± 0.0        | 1.20 ± 0.45     |              |         |
| P <sub>1</sub>          |                 | <0.001*          | 0.034*  | 0.001*           | 0.082           |              |         |
| P <sub>2</sub>          |                 |                  | 0.042*  | 0.379            | 0.016*          |              |         |
| Sig. bet. grps.         |                 |                  | p <sub>3</sub> =0.250,p <sub>4</sub> =0.701,p <sub>5</sub> =0.125   |                  |                 |              |         |
| <b>Ground substance</b> |                 |                  |   |                  |                 |              |         |
| Min. – Max.             | 0.0 – 0.0       | 2.0 – 3.0        | 0.0 – 1.0   | 1.0 – 2.0        | 0.0 – 1.0       | H= 19.317*   | 0.001*  |
| Mean ± SD.              | 0.0 ± 0.0       | 2.60 ± 0.55      | 0.80 ± 0.45   | 1.20 ± 0.45      | 0.40 ± 0.55     |              |         |
| P <sub>1</sub>          |                 | <0.001*          | 0.083   | 0.014*           | 0.386           |              |         |
| P <sub>2</sub>          |                 |                  | 0.020*  | 0.110            | 0.001*          |              |         |
| Sig. bet. grps.         |                 |                  | p <sub>3</sub> =0.465,p <sub>4</sub> =0.386,p <sub>5</sub> =0.110   |                  |                 |              |         |
| <b>Collagen</b>         |                 |                  |   |                  |                 |              |         |
| Min. – Max.             | 0.0 – 0.0       | 2.0 – 3.0        | 1.0 – 2.0   | 1.0 – 2.0        | 1.0 – 1.0       | H= 20.539*   | <0.001* |
| Mean ± SD.              | 0.0 ± 0.0       | 2.60 ± 0.55      | 1.20 ± 0.45   | 1.40 ± 0.55      | 1.0 ± 0.0       |              |         |
| P <sub>1</sub>          |                 | <0.001*          | 0.019*  | 0.006*           | 0.051           |              |         |
| P <sub>2</sub>          |                 |                  | 0.034*  | 0.085            | 0.012*          |              |         |
| Sig. bet. grps.         |                 |                  | p <sub>3</sub> =0.696,p <sub>4</sub> =0.696,p <sub>5</sub> =0.434   |                  |                 |              |         |
| <b>Vascularity</b>      |                 |                  |   |                  |                 |              |         |
| Min. – Max.             | 0.0 – 0.0       | 2.0 – 3.0        | 2.0 – 3.0   | 2.0 – 3.0        | 2.0 – 3.0       | H= 16.181*   | 0.003*  |
| Mean ± SD.              | 0.0 ± 0.0       | 2.20 ± 0.45      | 2.60 ± 0.55   | 2.80 ± 0.45      | 2.80 ± 0.45     |              |         |
| P <sub>1</sub>          |                 | 0.048*           | 0.004*  | 0.001*           | 0.001*          |              |         |
| P <sub>2</sub>          |                 |                  | 0.351   | 0.162            | 0.162           |              |         |
| Sig. bet. grps.         |                 |                  | p <sub>3</sub> =0.641,p <sub>4</sub> =0.641,p <sub>5</sub> =1.000   |                  |                 |              |         |
| <b>Score</b>            |                 |                  |   |                  |                 |              |         |
| Min. – Max.             | 0.0 – 0.0       | 9.0 – 11.0       | 5.0 – 7.0   | 7.0 – 8.0        | 5.0 – 6.0       | F= 129.89*   | <0.001* |
| Mean ± SD.              | 0.0 ± 0.0       | 10.0 ± 1.0       | 6.0 ± 1.0   | 7.40 ± 0.55      | 5.40 ± 0.55     |              |         |
| P <sub>1</sub>          |                 | <0.001*          | <0.001*   | <0.001*          | <0.001*         |              |         |
| P <sub>2</sub>          |                 |                  | <0.001*   | <0.001*          | <0.001*         |              |         |
| Sig. bet. grps.         |                 |                  | p <sub>3</sub> =0.043*,p <sub>4</sub> =0.685,p <sub>5</sub> =0.002* |                  |                 |              |         |

**SD:** Standard deviation      **H:** H for Kruskal Wallis test, Pairwise comparison bet. each 2 groups was done using Post Hoc Test (Dunn's for multiple comparisons test)      **F:** F for ANOVA test, Pairwise comparison bet. each 2 groups was done using Post Hoc Test (Tukey)      **p:** p value for comparing between the different studied groups  
**p<sub>1</sub>:** p value for comparing between Group I and each other groups      **p<sub>2</sub>:** p value for comparing between Group II and each other groups      **p<sub>3</sub>:** p value for comparing between Group III and Group IV      **p<sub>4</sub>:** p value for comparing between Group III and Group V      **p<sub>5</sub>:** p value for comparing between Group IV and Group V      \*: Statistically significant at p ≤ 0.05

**Table 2:** Comparison between the different studied groups according to morphometric study.

| Morphometric              | Subgroup IA (n = 5) | Subgroup IB (n = 5) | Group II (n = 5) | Group III (n = 5) | Group IV (n = 5) | F     | p     |
|---------------------------|---------------------|---------------------|------------------|-------------------|------------------|-------|-------|
| <b>t (mm)</b>             |                     |                     |                  |                   |                  |       |       |
| Min. – Max.               | 4.07 – 5.29         | 4.33 – 5.64         | 4.52 – 5.86      | 4.11 – 5.94       | 4.08 – 5.76      | 0.202 | 0.935 |
| Mean ± SD.                | 4.67 ± 0.52         | 4.95 ± 0.57         | 4.92 ± 0.54      | 4.96 ± 0.68       | 4.82 ± 0.69      |       |       |
| <b>w (mm)</b>             |                     |                     |                  |                   |                  |       |       |
| Min. – Max.               | 5.66 – 7.31         | 5.94 – 7.19         | 5.05 – 7.25      | 5.48 – 7.03       | 5.37 – 7.46      | 0.230 | 0.918 |
| Mean ± SD.                | 6.39 ± 0.69         | 6.38 ± 0.55         | 6.01 ± 0.94      | 6.20 ± 0.59       | 6.24 ± 0.79      |       |       |
| <b>A (mm<sup>2</sup>)</b> |                     |                     |                  |                   |                  |       |       |
| Min. – Max.               | 16.85 – 24.94       | 17.19 – 24.22       | 16.74 – 24.98    | 16.93 – 25.03     | 17.77 – 24.31    | 0.046 | 0.996 |
| Mean ± SD.                | 20.26 ± 3.26        | 20.30 ± 2.78        | 20.60 ± 3.20     | 20.91 ± 3.33      | 20.82 ± 2.70     |       |       |

**SD:** Standard deviation      **F:** F for ANOVA test      **p:** p value for comparing between the different studied groups



**Table 3:** Comparison between the different studied groups according to biomechanical Fmax.

| Biomechanical Fmax (N) | Group I (n = 5) | Group II (n = 5) | Group III (n = 5)  | Group IV (n = 5) | Group V (n = 5) | F       | p       |
|------------------------|-----------------|------------------|--|------------------|-----------------|---------|---------|
| Min. – Max.            | 7.10 – 8.20     | 2.80 – 3.50      | 3.50 – 4.0   | 4.80 – 6.0       | 5.90 – 6.80     | 129.43* | <0.001* |
| Mean ± SD.             | 7.72 ± 0.43     | 3.10 ± 0.26      | 3.78 ± 0.19  | 5.36 ± 0.49      | 6.28 ± 0.37     |         |         |
| p <sub>1</sub>         |                 | <0.001*          | <0.001*  | <0.001*          | <0.001*         |         |         |
| p <sub>2</sub>         |                 |                  | 0.057  | <0.001*          | <0.001*         |         |         |
| Sig. bet. grps.        |                 |                  | p <sub>3</sub> <0.001*, p <sub>4</sub> <0.001*, p <sub>5</sub> =0.006* |                  |                 |         |         |

SD: Standard deviation

F: F for ANOVA test, Pairwise comparison bet. each 2 groups was done using Post Hoc Test (Tukey)

p: p value for comparing between the different studied groups

p<sub>1</sub>: p value for comparing between Group I and each other groupsp<sub>2</sub>: p value

for comparing between Group II and each other groups

p<sub>3</sub>: p value for comparing between Group III and Group IVp<sub>4</sub>: p value for comparing

between Group III and Group V

p<sub>5</sub>: p value for comparing between Group IV and Group V

\*: Statistically significant at p ≤ 0.05

## DISCUSSION

In the present work assessment of the effect of PRP and PTX either alone or in combination on the healing of acute Achilles tendon injury following surgical repair in adult male Albino rats was done. To the best of our knowledge, it is the first time in which the effect of both treatments combined was evaluated. A standard rat model of Achilles tendon injury was performed including *ex vivo* mechanical and histological assessments as well as in *vivo* functional assays to target both pre- and post-injury differences<sup>[9,27,38]</sup>. Surgical repair was done prior to PRP or PTX administration to simulate the actual management guidelines for acute Achilles tendon injury, where the mainstay treatment is surgical repair since conservative treatment usually resulted in higher re-rupture rates when compared to operative repair<sup>[39,40]</sup>.

A single dose of PRP (at the site of injury) was injected immediately following surgical repair which was proven previously by Parafioriti *et al.*<sup>[41]</sup> to provide faster and more efficient healing when compared to delayed injection<sup>[42]</sup>.

In the present study, based on both histological and morphometric findings, there was a marked improvement in the tendon structure following treatment with PTX and/or PRP when compared with the group that didn't receive any adjuvant treatment following surgical repair (group II). In addition, our study also suggested that the most significant effect on the healing of the acutely injured tendon was achieved when combining PTX with PRP following the standard surgical repair procedure. Structural improvement was further supported functionally by the biomechanical results.

Generally, tendons undergo healing through three overlapping phases, the first being the inflammatory phase which lasts from 1-7 days. This phase is characterized by inflammatory cell migration such as neutrophils and macrophages. The second phase is the proliferative phase which lasts for two weeks on average. It is characterized by tenoblastic migration. Tenoblasts are active tendon cells that are responsible for synthesis of collagen, proteoglycans and extracellular matrix<sup>[43]</sup>. Finally the remodeling phase which usually starts from the 3rd to 4th week onwards<sup>[44,45]</sup>. The 15th day post-injury was chosen in the present study to assess the healing process histologically since PRP

and PTX affect healing in the early two phases of healing according to previous studies<sup>[10,27]</sup>.

Postoperatively, the rats were allowed to move freely in the present study since early voluntary mobilization has been shown to improve tendon healing in the early stage by increasing migration of inflammatory cells. Moreover, in the late phase, the tendons exhibited a more mature structure with fiber bundles arranged parallelly with interposed tenocytes when compared to the immobilized group<sup>[46,47]</sup>.

Regarding assessment of the histological changes, most studies described histological parameters subjectively which may result in uncertainty and difficulty in data comparison. That's why Bonar scale, together with morphometric analysis, were used in this study to quantify the histological findings and render the interpretation of the results easier and more objective. The variables of Bonar score include tenocytes morphology, ground substance, collagen, and vascularity. Scoring system was performed by two blinded observers<sup>[48]</sup>.

In the present work, hypercellularity as well as increased tenoblastic activity manifested by rounded nuclei and basophilic cytoplasm (denoting cellular activity) were evident in the treated groups but with variable degrees being the most prominent in the PRP-treated groups. This increase in tenoblast population is a possible result of the rich content of growth factors in PRP such as platelet-derived growth factor (PDGF), epidermal growth factor (EGF), fibroblast growth factor (FGF), transforming growth factor beta 1 (TGFβ1), insulin-like growth factor 1 and 2 (IGF-1 & IGF-2), vascular endothelial growth factor (VEGF), basic fibroblast growth factor (bFGF) and hepatocyte growth factor (HGF)<sup>[28,49]</sup>. These factors bind to their specific transmembrane receptors activating an intracellular signal protein which results in the expression of a gene sequence that initiates cellular division<sup>[23]</sup>. This was in agreement with other studies, which indicated that upon injecting PRP in the tendon lesion, the local proliferation of the platelet-rich fibrin scaffold provided hemostasis and allowed the slow delivery of cytokines and growth factors from platelets and plasma<sup>[50-52]</sup>. This molecular pool influences the different stages of regeneration outlined as apoptosis/necrosis, innate immune response, angiogenesis, cell proliferation and differentiation and tissue remodeling

leading to diminished pain and swelling, and improved function that decreases the time required for restoration and rehabilitation<sup>[53,54]</sup>.

The present study showed a smaller number of mature tenocytes in the PTX-only-treated group than in PRP-treated groups, but still higher than the untreated group because PTX also increases the levels of TGFs such as bone morphogenetic protein 4 (BMP-4)<sup>[2]</sup>. The tendon cells showed more rounding of their nuclei than those in the PRP-treated groups (mean Bonar score = 2). The increased number of migrating tenoblasts caused the proliferative phase to be early initiated and the deposition of collagen fibers to increase. As a result, the remodeling phase also began earlier than in the injured untreated group.

In another study by Şahin *et al.*<sup>[2]</sup>, who used PTX as a healing booster, no significant difference in fibroblastic activity was identified between PTX-treated group and control group two weeks post-injury; however, the PTX group had a higher regular collagen fibers percentage.

Another element that possibly contributed to the hypercellularity observed in all groups, especially the PRP-treated groups is the possible activation of tendon-derived stem cells (TDSCs), which account for 1–4 % of all nucleated tendon cells<sup>[55,56]</sup>.

TDSCs are pluripotent cells that have been shown to differentiate into tissues like tendon, cartilage, bone, and tendon-bone junctions in animal models as well as into tenocytes, adipocytes chondrocytes, and osteocytes upon induction<sup>[56,57]</sup>.

TGF- $\beta$  has been shown to share in tendons development and healing. Thus, it is suggested that the TGF signaling pathway is responsible for TDSCs fate through the induction of Sclertaxis (Scx) expression, which has been proved as one of the main regulators of tendon development<sup>[55]</sup>. Since PRP is rich in growth factors among which TGF- $\beta$  family is present. So, it is hypothesized that PRP plays a role in stimulating the tendon stem cell niche, possibly contributing to better healing results in the PRP-treated groups.

In the present study, increased thickness of the paratenon, hypercellularity and neovascularization especially at the tendon-paratenon interface was observed in all the treated groups. This can be explained by the role of paratenon and paratenon-derived cells (PDCs) in the healing process<sup>[58]</sup>. Similar observations were found by Imai *et al.*<sup>[59]</sup> who suggested that during the initial phase of tendon repair, in *vitro* PRP therapy improved the tendon-healing properties of PDCs. They observed that PRP significantly enhanced the migration of PDCs to the injury site which accelerated healing in comparison to the untreated group.

Increased number of capillaries or neovascularization was observed in all groups that received treatment but was most evident in the PTX and combined group. This significant increase in neovascularization demonstrated in the PTX-treated groups could be attributed to PTX growth

factor stimulation, especially VEGF, which in turn may result in the acceleration of tendon healing<sup>[2,19]</sup>. In addition, PTX is a non-specific phosphodiesterase inhibitor that increases intracellular cyclic adenosine monophosphate (c-AMP) levels by inhibiting its breakdown by phosphodiesterases (PDEs)<sup>[60]</sup>. This effect improves tissue perfusion through vasodilatation, decreasing plasma viscosity thus improving vascularity of injured tissue<sup>[19]</sup>.

PRP promoted neovascularization especially in the early phase of tendon healing, where scattered capillaries have been observed in group III especially at the tendon-paratenon interface (mean Bonar score = 2.6). This can be explained by the liberation of stored angiogenic factors from the activated platelets. Similar results were reported by Genç *et al.*<sup>[61]</sup> who identified that low-perfusion areas like Achilles tendons benefit greatly from VEGF.

In the present study, an increase in inflammatory cell migration, tissue gaps, as well as thickening and edema of paratenon in the untreated injured group was observed compared to the treated groups due to the prolongation of the inflammatory phase in the untreated group. Meanwhile, the decreased inflammatory cellular infiltration observed in the treated groups could be due to the anti-inflammatory effect of both PRP and PTX through blocking inflammatory actions of interleukin-1 (IL-1) and tumor necrosis factor-alpha (TNF- $\alpha$ ) on neutrophils<sup>[62]</sup>. The inflammatory cell infiltration in the tendon tissue and the paratenon was much less in the PRP group than in PTX group. Moreover, the paratenon edema proved by the presence of tissue gaps between fibers was marked in the PTX-treated group more than the PRP-treated groups. Consequently, PRP has shown to be superior to PTX in its anti-inflammatory effect.

Another key event in the pathological process of tendon injury is lipid infiltration and adipocyte accumulation and may thereby increase the risk of tendon rupture in clinical practice. Hence, it is important to inhibit adipogenesis and accumulation of lipids in order to restore the structural and functional properties of the injured tendon<sup>[63]</sup>. In the present study, Adipocyte infiltration was obviously detected in the untreated group indicating the active pathological process and poorer healing. This adipose infiltration was almost absent in the treated groups either by PTX, PRP or combined. This gives another evidence of the improvement in the healing process using these treatments.

The regenerative potential of PRP & PTX was further supported by Masson's Trichrome stain results that revealed an improvement in the distribution of collagen fibers and intensity of staining in all treatment groups and were almost back to normal in the combined group. This can be explained by the fact that the growth factors in the PRP boost healing and regeneration through stimulation of cellular signaling pathways that promote angiogenesis, cell proliferation, cell differentiation, and matrix formation<sup>[41,42]</sup>.

Regarding the histological assessment of PTX effect on Achilles tendon injury, the present study showed positive effects of PTX on the healing process of the injured



tendons. In a previous study performed by Palabıyık *et al.*<sup>[20]</sup>, PTX showed favorable results of modified Movin & Bonar scoring system when compared to the control in terms of vascularity, inflammation, collagen organization, chondroid metaplasia, osseous metaplasia, hyalinization and round cells. This effect is mainly due to that PTX increases the levels of BMP-4 which plays an important role in the tendon healing process. Moreover, PTX inhibits the inflammatory process by reducing TNF- $\alpha$ , IL-1 and IL-6 levels<sup>[64]</sup>.

In the present study, a combined Alcian blue/PAS staining technique was used to stain the ground substance between collagen fibers. PAS was used as a counter stain to allow better visualization of the stained matrix<sup>[65]</sup>. According to Bonar score, the higher the intensity of the Alcian blue stain, the less the healing of the tendon<sup>[48]</sup>. PRP-treated groups showed minimal ground substance deposition between fibers (mean Bonar score = 0.8) when compared to untreated group.

Scanning electron microscope (SEM) results came in accordance with Masson's trichrome results. PRP-treated groups showed more deposition of mature collagen, axialization of collagen fibers, and less tissue gaps than all other experimental groups. On the other hand, untreated group II showed thin randomly oriented branched loosely arranged immature collagen fibers giving a lacy appearance. During the proliferative phase of healing, tenoblasts secrete immature collagen type III fibers which are replaced by collagen type I during the remodeling phase<sup>[43,45,66]</sup>.

Scanning electron microscope examination of PTX-treated group despite showing superior results to untreated positive control group in terms of collagen axialization, mature to immature collagen ratio and tissue gaps, it was still inferior to the PRP-treated groups.

Regarding assessment of the combined treatment, group V showed better histological features than either treatment alone. There was an evident restoration of normal tissue architecture superior to all other treated groups approaching the control group. Collagen fibers appeared well organized and axialized in H & E sections (mean Bonar score = 1). This was confirmed by Masson's trichrome and SEM. There have been minimal tissue gaps between fibers. Inflammatory cell infiltration was minimal. Hypercellularity was significant with tendon cells nuclei appearing more fusiform to spindle in shape (mean Bonar score = 1.2). Minimal ground substance deposition between fibers denoting better healing (mean Bonar score = 0.4). Neovascularization was evident at tendon paratenon interface (mean Bonar score = 2.8). The mean of the overall Bonar score was 5 which is less than all other treated groups. All these observations denote that combined treatment PRP and PTX has a potentially better healing effect on injured Achilles tendon.

The gross morphological assessment in the present study showed statistically non-significant differences

between the treated groups and the control group regarding the tendon width, thickness and cross-sectional area at day 30 post-injury. These results agree with that of Kaux *et al.*<sup>[67]</sup>, since the cross-sectional area of tendons in the control group was similar to that of PRP-treated group 30 days post-injury. Similar results were obtained from another study where tendon diameter in PRP-treated groups had a slight increase compared to the control group, however, these changes weren't significant<sup>[68]</sup>. Based on this evidence, we can conclude that morphological assessment alone is not a reliable tool to assess healing.

In the present work, biomechanical test was performed on the 30th day post-injury to allow enough remodeling of the injured tendons to withstand the tension force. Tendons treated with PRP and PTX show superior biomechanical properties in terms of tensile strength and load to failure (Fmax). This proves the better remodeling of the treated tendons over the control. A combination of both PTX and PRP had a better result than either alone, which proves a synergism between these two treatments for better functional outcomes post-healing.

The obtained results from the present study agree with that of YkSel *et al.*<sup>[27]</sup> where Fmax values of the PRP-treated group approached those of the control 30 days post-injury. Moreover, in the study performed by Takamura *et al.*<sup>[2]</sup>, PTX-treated group showed higher maximum rupture force as well as higher maximum displacement than in the control group. Contrarily, Gen *et al.*<sup>[61]</sup> found that biomechanical analyses did not reveal significant differences between treated groups. The same result was obtained in the study performed by Circi *et al.*<sup>[42]</sup> This controversy could be explained by the small sample size used in these previously mentioned studies.

## CONCLUSION

There is a significant benefit of using PRP and PTX either alone or in combination in promoting Achilles tendon healing post-injury. PTX has shown to be of significant value both histologically & biomechanically in boosting the healing process in acute Achilles tendon injury; however, it was less effective than PRP. Combination of both treatments is of a better value than either treatment alone which suggests a synergistic effect between both treatments. The difference between groups regarding the gross morphology of the tendons post-healing is non-significant.

## CONFLICT OF INTERESTS

There are no conflicts of interest.

## REFERENCES

1. elik M, Bayrak A, Duramaz A, Bařaran SH, Kızılkaya C, Kural C, *et al.* The effect of fibrin clot and C vitamin on the surgical treatment of Achilles tendon injury in the rat model\*. *Foot Ankle Surg.* 2021;27(6):681–7.

2. Şahin AA, Özturan KE, Çiraklı A, Yılmaz F, Boz M, Kizilay H. The effect of pentoxifylline on Achilles tendon healing in tenotomized rabbits. *Eklemler Hastalıkları ve Cerrahisi*. 2019;30(3):259–66.
3. Tempfer H, Kaser-Eichberger A, Lehner C, Gehwolf R, Korntner S, Kunkel N, *et al.* Bevacizumab Improves Achilles Tendon Repair in a Rat Model. *Cell Physiol Biochem*. 2018;46(3):1148–58.
4. Dincel YM, Adanir O, Arikan Y, Çağlar AK, Doğru SC, Arslan YZ. Effects of high-dose vitamin C and hyaluronic acid on tendon healing. *Acta Ortop Bras*. 2018;26(2):82–5.
5. Güngörmüş C, Kolankaya D, Aydın E. Histopathological and biomechanical evaluation of tenocyte seeded allografts on rat Achilles tendon regeneration. *Biomaterials*. 2015;51:108–18.
6. Padilla S, Sánchez M, Vaquerizo V, Malanga GA, Fiz N, Azofra J, *et al.* Platelet-rich plasma applications for achilles tendon repair: A bridge between biology and surgery. *Int J Mol Sci*. 2021;22(2):1–17.
7. Galanty HL, Bradley JP. Achilles tendon ruptures. *Top Emerg Med*. 1995;17(2):36–46.
8. Nicodemo M de C, Das Neves LR, Aguiar JC, Brito F de S, Ferreira I, Sant'Anna LB, *et al.* Amniotic membrane as an option for treatment of acute achilles tendon injury in rats. *Acta Cir Bras*. 2017;32(2):125–39.
9. Greimers L, Drion P V, Colige A, Libertiaux V, Denoël V, Lecut C, *et al.* Effects of allogeneic platelet-rich plasma (PRP) on the healing process of sectioned achilles tendons of rats: A methodological description. *J Vis Exp*. 2018;2018(133):1–9.
10. Virchenko O, Aspenberg P. How can one platelet injection after tendon injury lead to a stronger tendon after 4 weeks? Interplay between early regeneration and mechanical stimulation. *Acta Orthop*. 2006;77(5):806–12.
11. Dietrich F, L Duré G, P Klein C, F Bampi V, V Padoin A, D Silva V, *et al.* Platelet-Rich Fibrin Promotes an Accelerated Healing of Achilles Tendon When Compared to Platelet-Rich Plasma in Rat. *World J Plast Surg [Internet]*. 2015;4(2):101–9.
12. Soliman MM, Zakaria MM, Nadim HS, El-Fakharany WA, Shokry MM, Sadek AS. Platelet-Rich Plasma Attenuates Isoproterenol-Induced Myocardial Injury in Adult Male Albino Rat: Histological and Immunohistochemical study. *Egyptian Journal of Histology*. 2023 Apr 2.
13. de Mos M, van der Windt AE, Jahr H, van Schie HTM, Weinans H, Verhaar JAN, *et al.* Can platelet-rich plasma enhance tendon repair? A cell culture study. *Am J Sports Med*. 2008 Jun;36(6):1171–8.
14. AHamid MS, MohamedAli MR, Yusof A, George J, Lee LPC. Platelet-rich plasma injections for the treatment of hamstring injuries: a randomized controlled trial. *Am J Sports Med*. 2014 Oct;42(10):2410–8.
15. Sanchez M. *American Journal of Sports*. 2014;(May).
16. Ahmed A, Gamal S, Ibrahim Ismail D, Filobos S. Histological Study on the Possible Role of Platelet Rich Plasma in Repair of induced Acute Skeletal Muscle Injury in Adult Male Albino Rats. *Egyptian Journal of Histology*. 2024 Jun 1;47(2):632–45.
17. Chen X, Jones IA, Park C, Vangsness CTJ. The Efficacy of Platelet-Rich Plasma on Tendon and Ligament Healing: A Systematic Review and Meta-analysis With Bias Assessment. *Am J Sports Med*. 2018 Jul;46(8):2020–32.
18. Moraes VY, Lenza M, Tamaoki MJ, Faloppa F, Belloti JC. Platelet-rich therapies for musculoskeletal soft tissue injuries. *Cochrane database Syst Rev*. 2013 Dec;(12):CD010071.
19. Abdel-Salam OME, Baiuomy AR, El-Shenawy SM, Arbid MS. The anti-inflammatory effects of the phosphodiesterase inhibitor pentoxifylline in the rat. *Pharmacol Res*. 2003;47(4):331–40.
20. Palabıyık MT, Akalın Y, Yalçın Ö, Şahin İG, Çevik N, Öztürk A. The effect of pentoxifylline and hyperbaric oxygen on achilles osteotendinous junction injury: An experimental animal model study. *Ortop Traumatol Rehabil*. 2019;21(6):435–42.
21. Dietrich F, Hammerman M, Blomgran P, Tötting L, Bampi VF, Silva JB, *et al.* Effect of platelet-rich plasma on rat Achilles tendon healing is related to microbiota. *Acta Orthop*. 2017;88(4):416–21.
22. Croisé B, Paré A, Joly A, Louisy A, Laure B, Goga D. Optimized centrifugation preparation of the platelet rich plasma: Literature review. *J Stomatol Oral Maxillofac Surg*. 2020;121(2):150–4.
23. Dhurat R, Sukesh M. Principles and methods of preparation of platelet-rich plasma: A review and author's perspective. *J Cutan Aesthet Surg*. 2014;7(4):189.
24. Shin H-S, Woo H-M, Kang B-J. Optimisation of a double-centrifugation method for preparation of canine platelet-rich plasma. *BMC Vet Res*. 2017;13(1):1–8.
25. Avcı S, Gungor H, Kumru AS, Şahin M, Gezer A, Gök U. Effects of Apixaban, Rivaroxaban, Dabigatran and Enoxaparin on Histopathology and Laboratory Parameters in Achilles Tendon Injury: An *in vivo* Study. 2021;(July).
26. Waite ME, Tomkovich A, Quinn TL, Schumann AP, Dewberry LS, Totsch SK, *et al.* Efficacy of common analgesics for postsurgical pain in rats. *J Am Assoc Lab Anim Sci*. 2015;54(4):420–5.

27. Yüksel S, Adanir O, Gültekin MZ, Çağlar A, Küçükylidirim BO, Güleç MA, *et al*. Effect of platelet-rich plasma for treatment of Achilles tendons in free-moving rats after surgical incision and treatment. *Acta Orthop Traumatol Turc*. 2015;49(5):544–51.
28. Patel NN, Labib SA, Dhurat R, Sukesh M, Abdel-Salam OME, Baiuomy AR, *et al*. The effect of fibrin clot and C vitamin on the surgical treatment of Achilles tendon injury in the rat model\*. *Acta Orthop Traumatol Turc [Internet]*. 2018;14(1):1–12.
29. Beytemür O, Yüksel S, Tetikkurt ÜS, Genç E, Olcay E, Güleç A. Isotretinoin induced achilles tendinopathy: Histopathological and biomechanical evaluation on rats. *Acta Orthop Traumatol Turc [Internet]*. 2018;52(5):387–91.
30. Aydin BK, Altan E, Acar MA, Erkoçak ÖF, Ugraş S. Effect of Ankaferd blood stopper® on tendon healing: An experimental study in a rat model of Achilles tendon injury. *Eklemler Hast ve Cerrahisi*. 2015;26(1):31–7.
31. Jeffree CE, Read ND. Ambient-and low-temperature scanning electron microscopy. *Electron Microscop. plant cells*. 1991;313:413.
32. Tahmasebi P, Javadpour F, Sahimi M. Three-dimensional stochastic characterization of shale SEM images. *Transp Porous Media*. 2015;110(3):521–31.
33. Zhang H-T, Ding J, Chow G-M. Morphological control of synthesis and anomalous magnetic properties of 3-D branched Pt nanoparticles. *Langmuir*. 2008;24(2):375–8.
34. Hayes A, Easton K, Devanaboyina PT, Wu JP, Kirk TB, Lloyd D. A review of methods to measure tendon dimensions. *J Orthop Surg Res*. 2019;14(1):1–12.
35. Kang SH, Choi MS, Kim HK, Kim WS, Bae TH, Kim MK, *et al*. Polydeoxyribonucleotide improves tendon healing following achilles tendon injury in rats. *J Orthop Res*. 2018;36(6):1767–76.
36. Kirkpatrick , Feeney, Brooke C., LA. A simple guide to IBM SPSS statistics for version 20.0. Belmont, Calif.: Wadsworth, Cengage Learning; 2013.
37. Altman DG, Bland JM. Improving doctors' understanding of statistics. *J R Stat Soc Ser A (Statistics Soc)*. 1991;154(2):223–48.
38. Abdel-Salam OME, Baiuomy AR, El-Shenawy SM, Arbid MS, Mohamad S, Shuid AN, *et al*. Effects of allogeneic platelet-rich plasma (PRP) on the healing process of sectioned achilles tendons of rats: A methodological description. *J Orthop Res [Internet]*. 2015;4(1):101–9.
39. Park SH, Lee HS, Young KW, Seo SG. Treatment of acute achilles tendon rupture. *CiOS Clin Orthop Surg*. 2020;12(1):1–8.
40. Soroceanu A, Glazebrook M, Sidhwa F, Aarabi S, Kaufman A. Surgical versus nonsurgical treatment of acute achilles tendon rupture: A meta-analysis of randomized trials. *J Bone Jt Surg*. 2012;94(23):2136–43.
41. Parafioriti A, Armiraglio E, Del Bianco S, Tibalt E, Oliva F, Berardi AC. Single injection of platelet-rich plasma in a rat Achilles tendon tear model. *Muscles Ligaments Tendons J*. 2011;1(2):41–7.
42. Çirci E, Akman YE, Sükür E, Bozkurt ER, Tüzüner T, Öztürkmen Y. Impact of platelet-rich plasma injection timing on healing of Achilles tendon injury in a rat model. *Acta Orthop Traumatol Turc*. 2016;50(3):366–72.
43. Rho JH, Ko IG, Jin JJ, Hwang L, Kim SH, Chung JY, *et al*. Polydeoxyribonucleotide ameliorates inflammation and apoptosis in achilles tendon-injury rats. *Int Neurolog J*. 2020;24(Suppl 2):S79–87.
44. Vasiliadis A V., Katakalos K. The role of scaffolds in tendon tissue engineering. *J Funct Biomater*. 2020;11(4).
45. Sasaki K, Yamamoto N, Kiyosawa T, Sekido M. The role of collagen arrangement change during tendon healing demonstrated by scanning electron microscopy. *J Electron Microscop (Tokyo)*. 2012;61(5):327–34.
46. Palmes D, Spiegel HU, Schneider TO, Langer M, Stratmann U, Budny T, *et al*. Achilles tendon healing: Long-term biomechanical effects of postoperative mobilization and immobilization in a new mouse model. *J Orthop Res*. 2002;20(5):939–46.
47. Godbout C, Ang O, Frenette J. Early voluntary exercise does not promote healing in a rat model of Achilles tendon injury. *J Appl Physiol*. 2006;101(6):1720–6.
48. Maffulli N, Longo UG, Franceschi F, Rabitti C, Denaro V. Movin and bonar scores assess the same characteristics of tendon histology. *Clin Orthop Relat Res*. 2008;466(7):1605–11.
49. Xu K, Al-ani MK, Sun Y, Xu W, Pan L, Song Y, *et al*. Platelet-rich plasma activates tendon-derived stem cells to promote regeneration of Achilles tendon rupture in rats. *J Tissue Eng Regen Med*. 2017;11(4):1173–84.
50. Hammond JW, Hinton RY, Curl LA, Muriel JM, Lovering RM. Use of autologous platelet-rich plasma to treat muscle strain injuries. *Am J Sports Med*. 2009 Jun;37(6):1135–42.
51. Dumont NA, Wang YX, Rudnicki MA. Intrinsic and extrinsic mechanisms regulating satellite cell function. *Development*. 2015 May;142(9):1572–81.
52. Foster TE, Puskas BL, Mandelbaum BR, Gerhardt MB, Rodeo SA. Platelet-rich plasma: from basic science to clinical applications. *Am J Sports Med*. 2009 Nov;37(11):2259–72.



53. Malanga GA, Goldin M. PRP : review of the current evidence for musculoskeletal conditions. 2014;1–15.
54. Grassi A, Napoli F, Romandini I, Samuelsson K, Zaffagnini S, Candrian C, *et al.* Is Platelet-Rich Plasma (PRP) Effective in the Treatment of Acute Muscle Injuries? A Systematic Review and Meta-Analysis. *Sports Med.* 2018 Apr;48(4):971–89.
55. Silv U, Moreno P, Ar J. Tissue-Specific Stem Cell Niche. 2015;(October):313–26.
56. Lovati AB, Corradetti B, Lange Consiglio A, Recordati C, Bonacina E, Bizzaro D, *et al.* Characterization and differentiation of equine tendon-derived progenitor cells. *J Biol Regul Homeost Agents.* 2011;25(2 Suppl).
57. Yang J, Zhao Q, Wang K, Liu H, Ma C, Huang H, *et al.* Isolation and biological characterization of tendon-derived stem cells from fetal bovine. *Vitr Cell Dev Biol - Anim [Internet].* 2016;52(8):846–56. Available from: <http://dx.doi.org/10.1007/s11626-016-0043-z>
58. Müller SA, Evans CH, Heisterbach PE, Majewski M. The Role of the Paratenon in Achilles Tendon Healing: A Study in Rats. *Am J Sports Med.* 2018 Apr;46(5):1214–9.
59. Imai S, Kumagai K, Yamaguchi Y, Miyatake K, Saito T. Platelet-Rich Plasma Promotes Migration, Proliferation, and the Gene Expression of Scleraxis and Vascular Endothelial Growth Factor in Paratenon-Derived Cells In *Vitro*. *Sports Health.* 2019;11(2):142–8.
60. Mohamad S, Shuid AN, Mohamed N, Fadzilah FM, Mokhtar SA, Abdullah S, *et al.* The effects of alpha-tocopherol supplementation on fracture healing in a postmenopausal osteoporotic rat model. *Clinics.* 2012;67(9):1077–85.
61. Genç E, Yüksel S, Çağlar A, Beytemur O, Akif Güleç M. Comparison on effects of platelet-rich plasma versus autologous conditioned serum on achilles tendon healing in a rat model. *Acta Orthop Traumatol Turc.* 2020;54(4):438–44.
62. Babaei S, Bayat M, Nouruzian M, Bayat M. Pentoxifylline improves cutaneous wound healing in streptozotocin-induced diabetic rats. *Eur J Pharmacol [Internet].* 2013;700(1–3):165–72.
63. Wang Y, He G, Wang F, Zhang C, Ge Z, Zheng X, *et al.* Aspirin inhibits adipogenesis of tendon stem cells and lipids accumulation in rat injury tendon through regulating PTEN/PI3K/AKT signalling. *J Cell Mol Med.* 2019;23(11):7535–44.
64. Tsutsumimoto T, Wakabayashi S, Kinoshita T, Horiuchi H, Takaoka K. A phosphodiesterase inhibitor, pentoxifylline, enhances the bone morphogenetic protein-4 (BMP-4)-dependent differentiation of osteoprogenitor cells. *Bone.* 2002 Sep;31(3):396–401.
65. Maffulli N, Barrass V, Ewen S. Light Microscopic Histology of Achilles Tendon Ruptures: A Comparison with Unruptured Tendons. *Am J Sports Med.* 2000 Nov 1;28:857–63.
66. Philip J, Hackl F, Canseco JA, Kamel RA, Kiwanuka E, Diaz-Siso JR, *et al.* Amnion-derived multipotent progenitor cells improve achilles tendon repair in rats. *Eplasty [Internet].* 2013;13:e31.
67. Kaux JF, Drion P V., Colige A, Pascon F, Libertiaux V, Hoffmann A, *et al.* Effects of platelet-rich plasma (PRP) on the healing of Achilles tendons of rats. *Wound Repair Regen.* 2012;20(5):748–56.
68. Rajabi H, Sheikhan Shahin H, Norouzian M, Mehrabani D, Dehghani Nazhvani S. The Healing Effects of Aquatic Activities and Allogenic Injection of Platelet-Rich Plasma (PRP) on Injuries of Achilles Tendon in Experimental Rat. *World J Plast Surg [Internet].* 2015;4(1):66–73.

## المخلص العربي

## تأثير البلازما الغنية بالصفائح و / أو البنوكسي فيلين على إصابة وتر العرقوب المستحثة تجريبيا في ذكور الجرذان البيضاء البالغة

ادهم عبد الرحمن<sup>١</sup>، سلوي سعيد السبع<sup>١</sup>، ايمان العزب بحيري العزب<sup>١</sup>، سالي محمود محمد حسين عمر<sup>١</sup>،  
دينا محمد رستم<sup>٢</sup>

<sup>١</sup> قسم التشريح الأدمي وعلم الأجنة، <sup>٢</sup> قسم الهستولوجيا وبيولوجيا الخلية - كلية الطب - جامعة الاسكندرية

**الخلفية:** تعد إصابة وتر العرقوب شائعة جداً لدى الرجال الرياضيين في منتصف العمر. يعد الإصلاح الجراحي هو الخيار العلاجي الأنسب، ومع ذلك، تم اعتماد اساليب أخرى للعلاج. تحتوي البلازما الغنية بالصفائح الدموية على عوامل نمو والتي تساهم في اسراع عملية التئام وتجدد الانسجة. يحسن البنوكسي فيلين التئام الأنسجة من خلال توسيع الأوعية الدموية وزيادة تدفق الدم، بالإضافة الي خواصه المضادة للالتهاب.

**الهدف:** كان الهدف من هذا البحث هو دراسة تأثير البلازما الغنية بالصفائح الدموية والبنوكسي فيلين اما بمفردهما او معا على عملية التئام وتر العرقوب المصاب في ذكور الجرذان البيضاء البالغة من خلال الدراسة النسيجية و المورفولوجية و الميكانيكية الحيوية.

**المواد وطرق البحث:** خمسة وتسعون من ذكور الجرذان البيضاء البالغة. تم استخدام خمسة جرذان كمانحين للبلازما الغنية بالصفائح الدموية. تم تقسيم تسعين جرذاً إلى ٥ مجموعات ١٨ جرذا لكل مجموعة. المجموعة الاولى: المجموعة الضابطة، المجموعة الثانية: المجموعة الغير معالجة، المجموعة الثالثة: تلقت حقنا موضعيا من البلازما الغنية بالصفائح الدموية في مكان الجراحة، المجموعة الرابعة: تلقت حقن عضلي للبنوكسي فيلين يوميا، المجموعة الخامسة: تلقت كلا العلاجين البلازما الغنية بالصفائح الدموية و البنوكسي فيلين.

في اليوم الخامس عشر، تم تشريح وتر العرقوب لثمانية جرذان من كل مجموعة. تم استخدام خمسة أوتار في الدراسة المجهرية الضوئية، واستخدمت الثلاثة الأخرى في دراسة البنية الدقيقة عن طريق المجهر الإلكتروني الماسح. في اليوم الثلاثين، تم تشريح وتر العرقوب لعشرة جرذان من كل مجموعة. تم استخدام خمسة أوتار في الدراسة المورفولوجية، بينما تم استخدام الخمسة أوتار الأخرى في الدراسة الميكانيكية الحيوية لدراسة الخواص الوظيفية للوتر.

**النتائج:** أظهرت المجموعة الخامسة المعالجة بالبلازما الغنية بالصفائح الدموية والبنوكسي فيلين نتائج التئام أفضل من جميع المجموعات التجريبية الأخرى من الناحية النسيجية والميكانيكية الحيوية. كما أظهرت المجموعة الثالثة المعالجة بالبلازما الغنية بالصفائح الدموية التئاما أفضل من المجموعة الرابعة المعالجة بالبنوكسي فيلين والتي كانت بدورها متفوقة على المجموعة الثانية الغير معالجة.

**الاستنتاج:** هناك فائدة ذات دلالة إحصائية من استخدام البلازما الغنية بالصفائح الدموية و البنوكسي فيلين معاً افضل من كل منهما بمفرده في تعزيز التئام وتر العرقوب بعد الإصابة.